Supplementary Information (SI) for Journal of Materials Chemistry A.

Energy Storage Behavior of Side Chain-Engineered Si-Bridged Redox Active Donor-Acceptor Conjugated Polymers Operated in Organic Electrolytes

Subir K. Pati[1], *Sunita Muduli*[2], *Dhananjaya Patra*[1,*], *Shinbee Oh*[3], *Bumjoon J. Kim*[3], *Sabyashachi Mishra*[2,*], *and Sungjune Park*[1,*]

[1]School of Chemical Engineering, Sungkyunkwan University, Suwon 16419, Republic of Korea

[2]Department of Chemistry, Indian Institute of Technology, Kharagpur 721302, India

[3]Department of Chemical and Biomolecular Engineering, Korea Advanced Institute of Science and Technology (KAIST), Daejeon 34141, Republic of Korea

E-mail: itspilu@gmail.com, mishra@chem.iitkgp.ac.in, sungjunepark@skku.edu

Supporting Information

1. EXPERIMENTAL DETAILS

1.1 General information - Equipment and procedural details

1.1.1 Nuclear magnetic resonance spectroscopy (NMR)

^{1}H and ^{13}C NMR spectra were recorded from $CDCl_3$ solutions using a Bruker AVANCE 400 MHz spectrometer at a temperature of 298 K; chemical shifts are reported as δ values (ppm), for 1H-NMRs referenced to the residual solvent peaks (δ: 7.26 for $CDCl_3$) and ^{13}C-NMRs, spectra were referenced to the residual solvent peaks (δ: 77.16 for $CDCl_3$).

1.1.2 Mass Spectroscopy

The molecular mass of the monomers (M1-M3) was measured by using Gas Chromatography (GC-LC) mass spectrometer (Model: WATERS (XEVO TQ-S)).

1.1.3 Thermogravimetric analysis (TGA)

The thermogravimetric analysis (TGA) was conducted by Q400 (WATERS, USA) for all the co polymers which exhibited high thermal stability and the thermal decomposition temperature (T_d) at 5% weight loss are all above 350 °C.

1.1.4 Gel permeation chromatography (GPC)

Gel permeation chromatography (GPC) was obtained from the Waters (Alliance e2695) model used to determine the molecular weights of both the copolymers.

1.1.5 X-ray diffraction (XRD)

XRD measurement of the polymer powders were conducted on a Bruker D8 Powder diffractometer using Cu X-ray tube (2.2 KW) with maximum voltage 40 kV and power 40 mA in with the 2θ of 3° to 30°.

1.1.6 Field emission scanning electron microscopy (FE-SEM)

Field emission type scanning electron microscope (FE-SEM, Hitachi, S-4700) was used for the morphology analysis of the powder polymeric samples.

1.1.7 Field Emission transmission electron microscopy (FETEM)

The FETEM measurement was conducted on Cs corrected-Field Emission Transmission Electron Microscope JEOL (JEM-ARM200F).

1.2 Materials and synthesis details of monomers (M1-M3) and polymers (Si-BDT-NDI and **Si-BDT -PDI)**

All chemicals and solvents were purchased in reagent grade from Aldrich, ACROS, and TCI, except the catalysts $Pd(PPh_3)_4$, and $Pd_2(dba)_2$ which were obtained from Strem Chemicals. All the polymers are prepared under nitrogen environment using standard Schlenk line techniques and using anhydrous solvents, received from commercial sources (Aldrich). Purification of the intermediates by column chromatography techniques using silica gel (Merck, Kieselgel 60 63-200 MYM SC). The synthesis procedure of intermediate and Monomers are presented in scheme 1 and two A1-A2 polymers in Scheme 2. Intermidates **2** [S1] was prepared by our earlier reported procedure. Monomers **M1**[S2], **M1**[S3], and **M3** [S4] were prepared by minor modification procedures in the literatures.

2. Characterizations of electrochemical properties

The electrochemical tests of the **Si-BDT-NDI** and **Si-BDT -PDI** polymeric composite electrodes were performed by assembling the 3-electrode-cell setup, comprising the Ag/AgCl as the reference electrode, Pt as the counter electrode, and a working electrode was prepared using 80% of the synthesized materials (**Si-BDT-NDI** and **Si-BDT -PDI**), with 10% of conducting C-65 carbon and PVDF each, individually on preactivated carbon cloth. The synthesized polymeric materials were studied using organic electrolyte of 0.1M $TBAPF_6$ in acetonitrile (ACN). The mass loading on the carbon cloth was ~ 2 mg. Cyclic voltammetry (CV) and galvanic charge–discharge (GCD), Electrochemical Impedance Speactra (EIS) tests were carried out to determine the working potential windows, C_S values, solution resistance etc.

The value of specific capacity (Csp) was calculated by using the following equation[S5]:

$$\mathbf{C_{sp} = I\Delta t / m} \qquad \text{(S1)}$$

where C_{sp}, I/m, and Δt denote the specific capacity (C g^{-1}), applied current density (A g^{-1}), and discharge time (s), of the charge–discharge curve, respectively.

2.1 Design of asymmetric hybrid supercapacitor (AHSC) cell:

An AHSC device was fabricated using 2electrode-cell, with porous activated carbon (PAC) as the cathode and **Si-BDT -PDI** polymer as the anode. A Whatman filter paper dipped in nonaqueous 0.1M $TBAPF_6$ was used as a separator. The mass ratio of the positive electrode and negative electrode was optimized using a theory of charge balance.

$$\frac{q+}{q-} = \frac{m+}{m-} = \frac{Csp- \times \Delta V-}{Csp+ \times \Delta V+} \qquad \text{(S2)}$$

where, m+ and m− are active material masses, Csp+ and Csp− are specific capacitances, ΔV+ and ΔV− are potential ranges for the cathode and anode half cells.

The energy density (E_d) and power densities (P_d) were calculated for full cells by using following equations.

$$\text{Energy density (Wh kg}^{-1}\text{)} = \frac{Csp \times \Delta V}{7.2} \qquad \text{(S3)}$$

$$\text{Power density (W kg}^{-1}\text{)} = \frac{Ed \times 3600}{\Delta t} \qquad \text{(S4)}$$

3. Scheme 1. Synthesis of intermediates and monomers

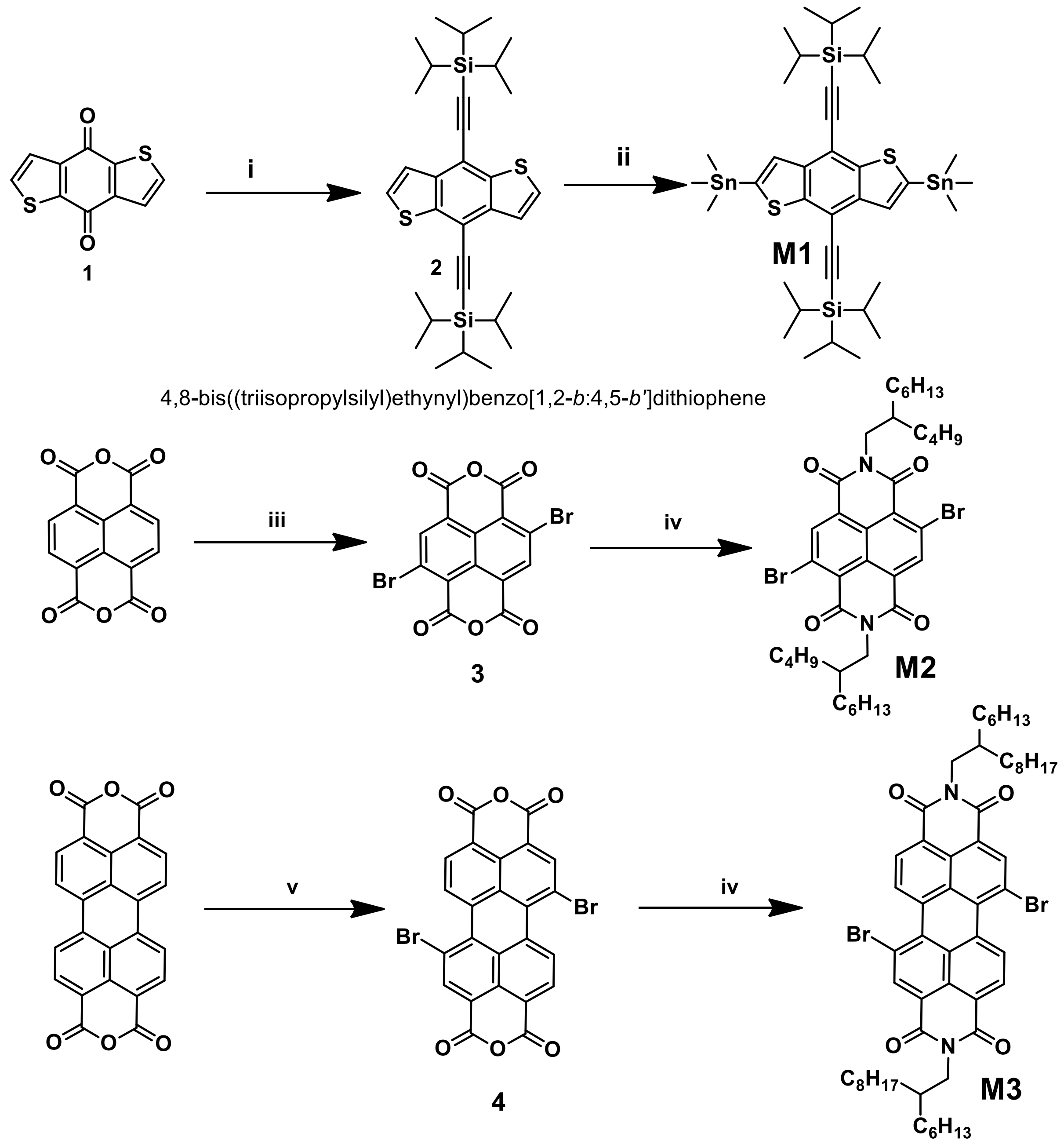

Reagents and conditions: (i) THF, BuLi, -78 °C, ethynyltriisopropylsilane; (ii) BuLi, -78 C, THF, $SnMe_3Cl$, (iii) 2- 2-decyltetradecan-1-amine, o-Xylene, Propionic Acid, 140 °C; (iv) Br_2, H_2SO_4, 85 °C.

Scheme 2. Synthesis of D-A based polymers (**Si-BDT-NDI** or **Si-BDT -PDI**).

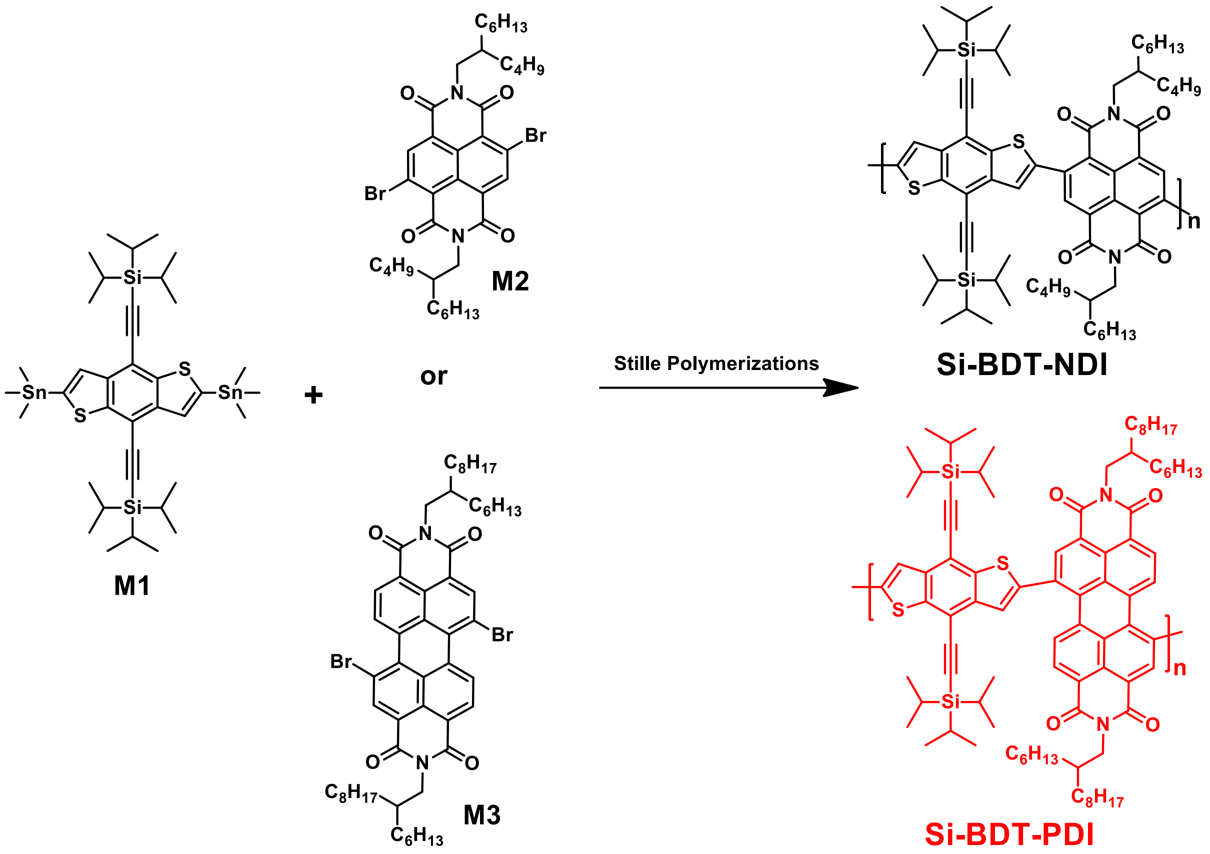

Stille polymerization conditions: P(*o*-tolyl)$_3$, CuI, Pd$_2$(dba)$_3$, and chlorobenzene at 130 °C for 24 hr.

4. Synthesis of intermediates, monomers (**M1-M3**) and polymers **(SiBDT-NDI** and **SiBDT-PDI)**

2,6-Bis(trimethyltin)-4,8-bis(triisopropylsilylethynyl)-benzo[1,2- b:4,5-b]dithiophene (M1)

To a flame dried a two neck round bottom flask with protection of argon, charged compound 2 (1.5 g 3.67 mmol), TMEDA (1.3 mL, 10.8 mmol) and THF (50 mL). Subsequently, the reaction mixture was cooled to -78 °C, for some time and 6.8 mL of n-BuLi (10.8 mmol, 1.6 M solution in hexanes) was added dropwise via syringe. After stirring at low temperature for 1h, 12.7 mL of trimethyltinchloride (12.7 mmol, 1.0 M solution in hexane) was added in one portion. The reaction mixture wasallowed to warm to room temperature overnight. The reaction mixture was quenched with water then washed with water and brine and the organic layer was dried over magnesium sulfate and concentrated via rotary evaporation. Crude compound was recrystallized with isopropyl alcohol to yield a pale yellow solid (2.46 g, 80%). ^{1}H-NMR (400 MHz, $CDCl_3$) δ (ppm) 7.68 (s, 2H), 1.32, (m, 6),1.23 (m, 36H). 0.47 (s, 18H). ^{13}C NMR (75 MHz, $CDCl_3$) δ (ppm) 144.68, 143.51, 139.63, 131.10, 110.36, 103.33, 100.64, 18.86, 11.38, -8.37. GC-MS: m/z: 876.18. Anal. calcd for [$C_{38}H_{62}S_2Si_2Sn_2$]: C, 52.06; H, 7.13; S, 7.32. Found: C, 52.10; H, 7.11; S, 7.27%.

2,6-dibromonaphthalene-1,4,5,8-tetracarboxydianhydride (3)

1,4,5,8-naphthalenetetracarboxylic dianhydride (2.0 g, 7.5 mmol) and oleum (20% SO_3, 70 mL) charged to a flame dried a two neck round bottom flask and stirred at 55 ^{o}C for 2 hours. A solution of dibromoisocyanuric acid (2.2 g, 7.7 mmol) in oleum (40 mL) was then added drop wise over a period of 30 mins. The resulting mixture was then heated to 85 ^{o}C and maintained at this temperature for 2 days. Upon cooling to room temperature, the reaction mixture was poured slowly into crushed ice (300 g). Subsequently the mixture was diluted with water (300 mL) and then stirred at room temperature for 1 hour. The precipitates were collected by filtration, washed with water, hexane, and methanol, and dried under vacuum, offering greenish yellow solid (2.5 g, 5.87 mmol, yield 78.2%). This product was used to the next step without any further purification.

N,N'-bis(2-butyloctyl)-2,6-dibromonaphthalene-1,4,5,8- bis(dicarboximide) (M2)

To a flame dried a two neck round bottom flask charged compound 3 (2.0 g, 4.69 mmol), 2- 2-2-butyloctan-1-amine (2.61 g, 14.08 mmol), o-xylene (1 mL), and propionic acid (5 mL), the resulting mixture was stirred at 140 ^{o}C for 2 h. After cooling to room temperature, the solvents were removed in vacuo, and the residue was purified by column chromatography on silica gel with a mixture of chloroform:hexane (1:3, v/v) as eluent. The resulting product was an off-white solid with a yield of 1.46 g, 40.9%. ^{1}H-NMR (400 MHz, $CDCl_3$, δ) 8.98 (s, 2H), 4.14 (d, J = 4 Hz, 2H), 1.98 (m, 2H), 1.39-1.24 (m, 32H), 0.89-0.83 (m, 12H). ^{13}C-NMR (100 MHz, $CDCl_3$, δ) 161.18, 161.03, 139.14, 128.25, 127.76, 125.30, 124.11, 45.43, 36.18, 31.80, 31.56, 31.26, 28.54, 26.54, 26.31, 29.61, 23.06, 22.63, 14.05. GC-MS: m/z: 761.03. Elemental analysis calculated for [$C_{38}H_{52}Br_2N_2O_4$]: C, 60.00; H, 6.89; Br, 21.01; N, 3.68; O, 8.41 Obtained: C, 59.81; H, 6.79, N, 3.86.

5,12-dibromoanthra[2,1,9-def:6,5,10-d'e'f']diisochromene-1,3,8,10-tetraone (4)

A mixture of perylenetetracarboxylic dianhydride (PTCDA) (20.0 g, 51 mmol) and sulfuric acid (200 mL, 96%) was stirred overnight at room temperature and subsequently iodine (0.0 g, 2.0 mmol) was added. The temperature of the reaction mixture was kept at 85 °C, followed by dropwise addition of bromine (18.8 g, 6.0 mL, 117.3 mmol) over a period of 1 h. The reaction mixture was allowed to heat overnight at the same temperature and then cooled down to room temperature. An air stream was passed into the reaction to remove the excess bromine fumes. Water (65 mL) was added to the reaction and the resulting precipitate was separated by Buchner filtration, washed with sulfuric acid (86 %, 200 ml) and an excess amount of water, acetone (about 50 mL), and dried in vacuum to result dibromo the product. Yield = 40 gm (88 %). This product was used to the next step without any further purification.

N,N′-Bis(2-hexyldecyl)-2,8-dibromo-3,4,9,10-perylene tetracarboxylicdiimide (M3) :

To the mixture of compound 4 (2.1 g, 3.81 mmol), 2-hexyldecan-1-amine (2.76 g, 11.43 mmol), o-xylene (12 mL), and propionic acid (4 mL) was stirred in a two neck round bottomed flask at 140 ^{o}C for 2 h. Later in the reaction was cooling to room temperature, the solvents were removed in vacuo, and the residue was purified by column chromatography on silica gel with a mixture of chloroform:hexane (1:1, v/v, gradually up to 3:2) as eluent, resulting a red solid powder (2.91 g, 2.91 mmol, yield 76.3%). ^{1}H-NMR (400 MHz, $CDCl_3$, δ) 9.42 (d, J = 8.0 Hz, 2H), 8.86 (s, 2H), 8.64 (d, J = 8.0 Hz, 2H), 4.13 (d, J = 7.2 Hz, 4H), 2.0-1.98 (m, 2H), 1.4-1.25 (m, 48H), 0.86-0.82 (m, 12H). ^{13}C-NMR (100 MHz, $CDCl_3$, δ) 163.19, 162.69, 138.05, 132.87, 132.74,130.03, 129.19, 128.44, 126.93, 123.14, 122.72, 120.80, 44.86, 36.63, 31.39, 31.91, 31.69, 30.05, 29.67, 29.65, 29.60, 29.36, 29.33, 26.50, 22.64, 14.13. GC-MS: m/z: 996.70.. Elemental analysis calculated for [$C_{56}H_{72}Br_2N_2O_4$]: C, 67.46; H, 7.28; Br, 16.03; N, 2.81; O, 6.42. Obtained: C, 67.44; H, 7.24; N, 2.92.

General procedure for the synthesis of two D-A copolymers (SiBDT-NDI or **SiBDT-PDI)**.

To a 20 ml clean and dry microwave vial were charged with monomer **M1** (0.150 mmol), monomer **M2** or **M3**, (0.150 mmol), $Pd_2(dba)_3$ (0.005 g, 0.005 mmol), $P(o\text{-tolyl})_3$ (0.006 g, 0.02 mmol), and CuI (0.004g, 0.02 mmol). The sealed microwave vial was applied with three cycles of vacuum and purge N_2 and then added chlorobenzene (5 mL) was kept at 130 °C for 48 hr. After cooling to room temperature, the reaction mixture was added dropwise into a mixture of hydrochloric acid (1N, 10 mL) and methanol (200 mL) and stirred for 2 hrs. The polymer precipitate was filtered through a thimble and purified with Soxhlet extraction using each solvent methanol, acetone, hexane, dichloromethane, and chloroform for 24 hr. The chloroform soluble fraction was concentrated and reprecipitated into methanol, filtered, and dried under a vacuum at 100 °C to achieve the desired polymers. as a dark solid.

Poly-{2,7-bis(2-butyloctyl)-4-methyl-9-(6-methyl-4,8-bis((triisopropylsilyl)ethynyl)benzo[1,2-b:4,5-b']dithiophen-2-yl)benzo[lmn][3,8]phenanthroline-1,3,6,8(2H,7H)-tetraone} **(Si-BDT-NDI)**: using monomer M1 (122.5 mg) and M2 (114.1 mg), Yield = 94 mg, 58%. GPC: Mn = 36.1 K Da, PDI (Đ) = 1.98. ^1H NMR (400 MHz, $CDCl_3$, δ) 8.94 (br), 7.69 (br), 4.10 (br), 1.98 (br), 1.54-1.17 (br), 0.88-0.80 (br).

Poly-{2,9-bis(2-hexyldecyl)-5-methyl-12-(6-methyl-4,8-bis((triisopropylsilyl)ethynyl)benzo[1,2-b:4,5-b']dithiophen-2-yl)anthra[2,1,9-def:6,5,10-d'e'f']diisoquinoline-1,3,8,10(2H,9H)-tetraone compound with methane (1:1)} **(Si-BDT-PDI)**: using monomer M1 (140.2 mg) and M3 (149.5 mg), Yield = 138 mg, 65%, GPC: M_n =38.0 K Da, PDI (Đ) =1.44. ^1H NMR (400 MHz, $CDCl_3$, δ) 8.90 (br), 8.46-8.36 (br), 7.89 (br), 4.14 (br), 2.04 (br), 1.25-1.16 (br), 1.10-1.86 (br).

(a)

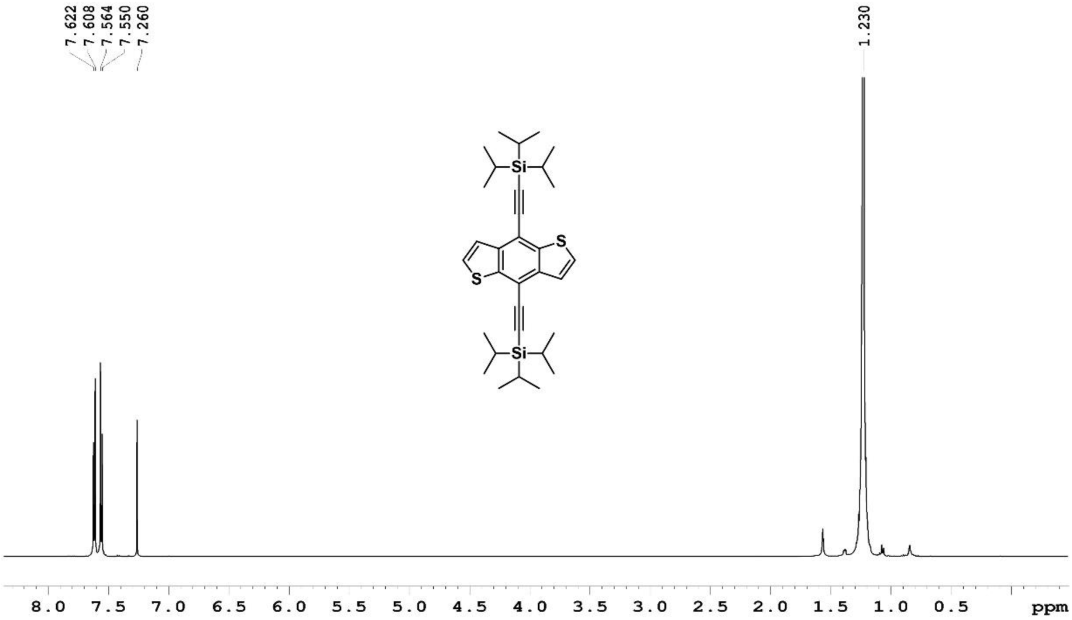

(b)

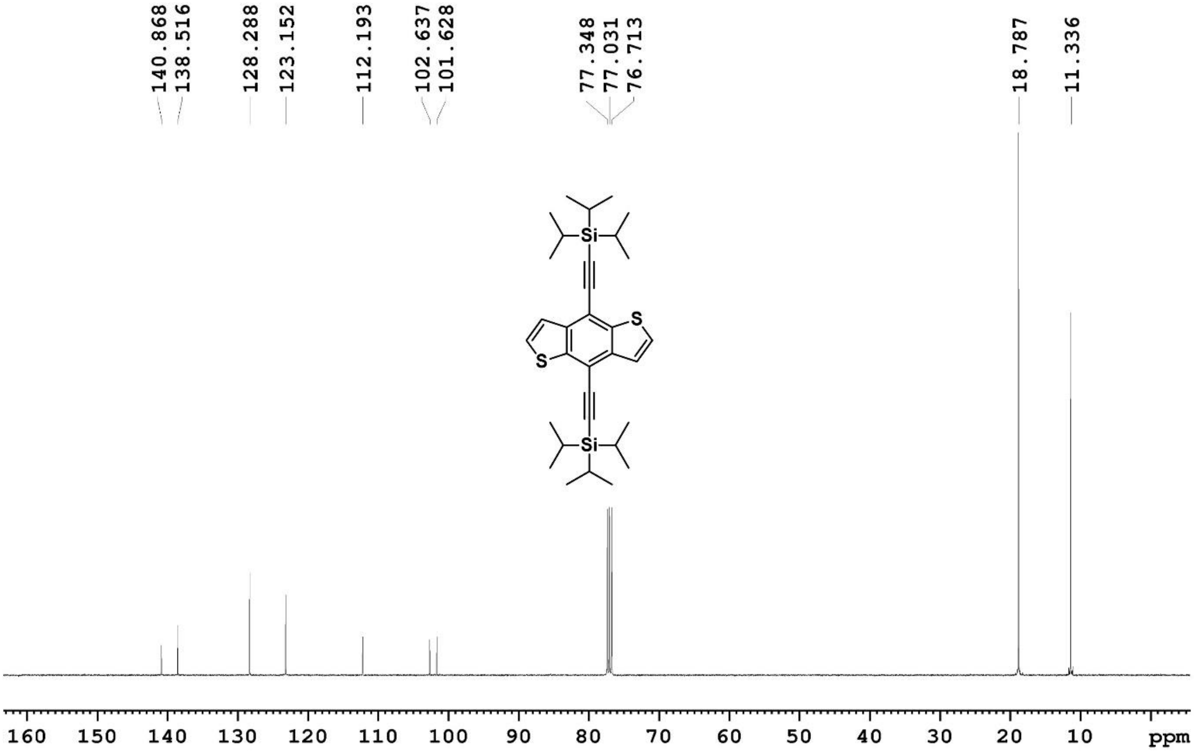

Figure S1. (a) ^{1}H- and (b) ^{13}C-NMR spectra of intermediate M1 in $CDCl_3$.

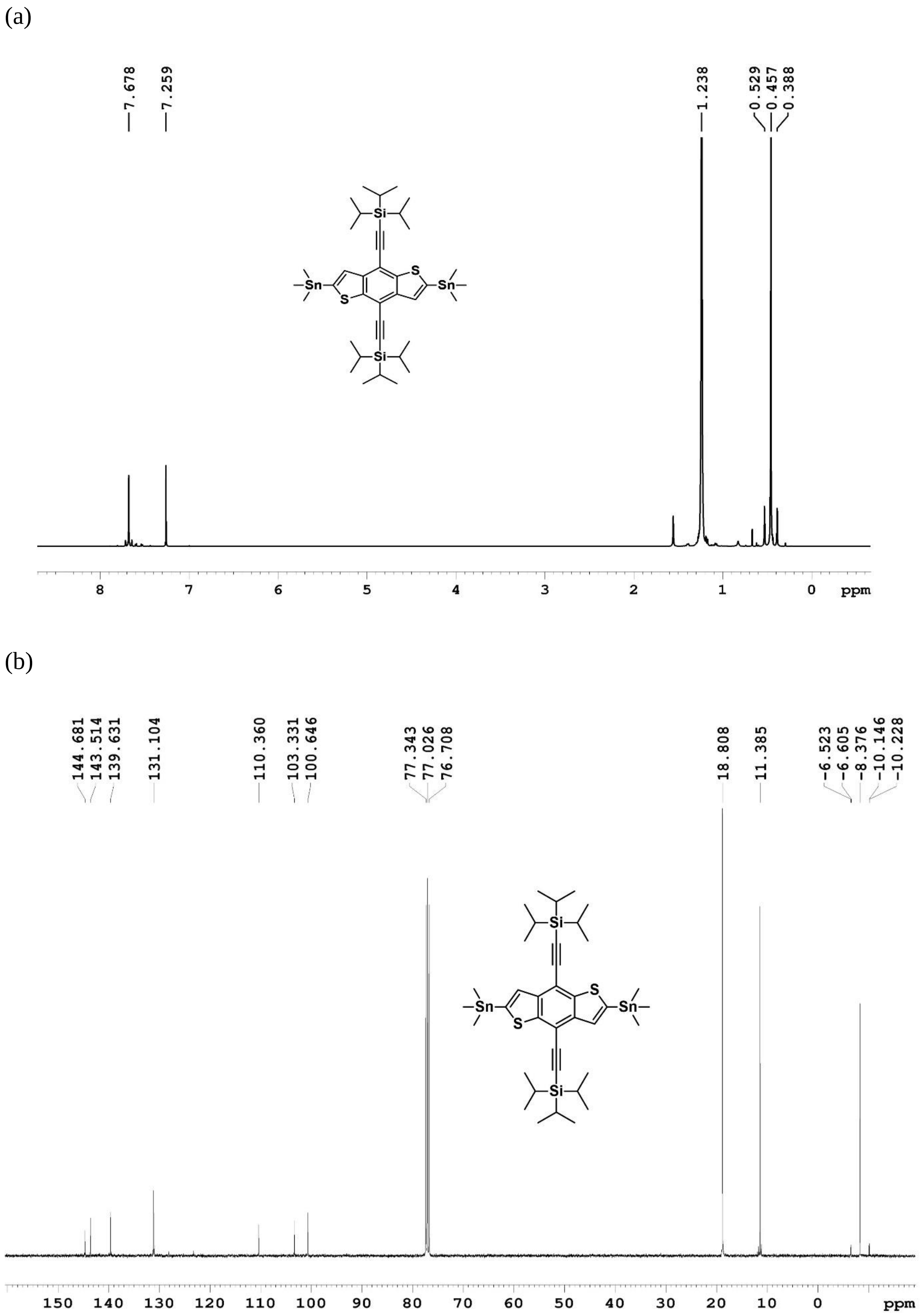

Figure S2. (a) ^{1}H- and (b) ^{13}C-NMR spectra of monomer M1 in $CDCl_3$.

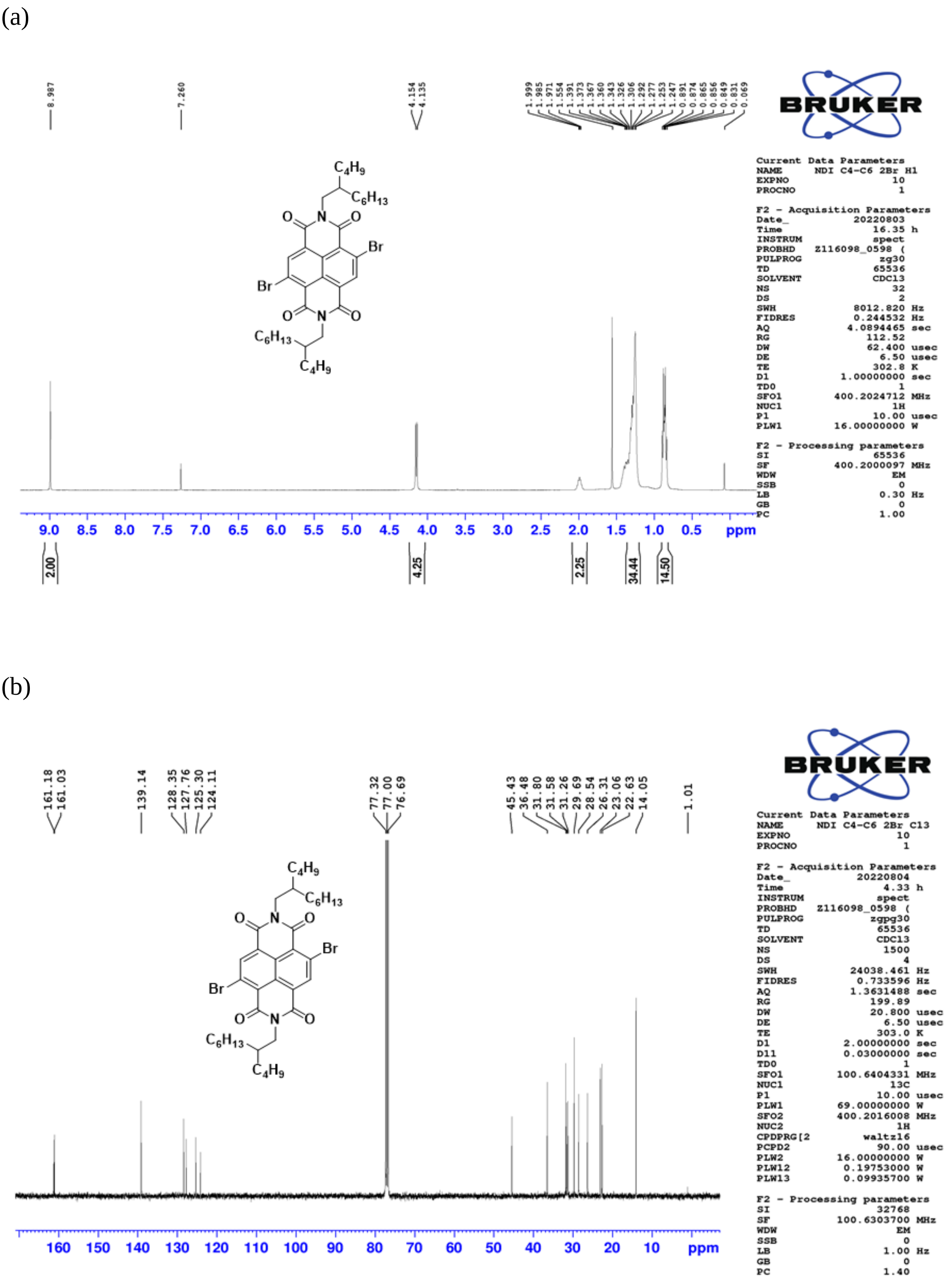

```
Current Data Parameters
NAME        NDI C4-C6 2Br H1
EXPNO                     10
PROCNO                     1

F2 - Acquisition Parameters
Date_               20220803
Time                 16.35 h
INSTRUM                spect
PROBHD     Z116098_0598 (
PULPROG                 zg30
TD                     65536
SOLVENT                CDCl3
NS                        32
DS                         2
SWH                 8012.820 Hz
FIDRES              0.244532 Hz
AQ                 4.0894465 sec
RG                    112.52
DW                    62.400 usec
DE                      6.50 usec
TE                     302.8 K
D1                1.00000000 sec
TD0                        1
SFO1             400.2024712 MHz
NUC1                      1H
P1                     10.00 usec
PLW1             16.00000000 W

F2 - Processing parameters
SI                     65536
SF               400.2000097 MHz
WDW                       EM
SSB                        0
LB                      0.30 Hz
GB                         0
PC                      1.00
```

```
Current Data Parameters
NAME        NDI C4-C6 2Br C13
EXPNO                     10
PROCNO                     1

F2 - Acquisition Parameters
Date_               20220804
Time                  4.33 h
INSTRUM                spect
PROBHD     Z116098_0598 (
PULPROG               zgpg30
TD                     65536
SOLVENT                CDCl3
NS                      1500
DS                         4
SWH                24038.461 Hz
FIDRES              0.733596 Hz
AQ                 1.3631488 sec
RG                    199.89
DW                    20.800 usec
DE                      6.50 usec
TE                     303.0 K
D1                2.00000000 sec
D11               0.03000000 sec
TD0                        1
SFO1             100.6404331 MHz
NUC1                     13C
P1                     10.00 usec
PLW1             69.00000000 W
SFO2             400.2016008 MHz
NUC2                      1H
CPDPRG[2             waltz16
PCPD2                  90.00 usec
PLW2             16.00000000 W
PLW12             0.19753000 W
PLW13             0.09935700 W

F2 - Processing parameters
SI                     32768
SF               100.6303700 MHz
WDW                       EM
SSB                        0
LB                      1.00 Hz
GB                         0
PC                      1.40
```

Figure S3. ^{1}H- and ^{13}C-NMR spectra of monomer M2 in $CDCl_3$.

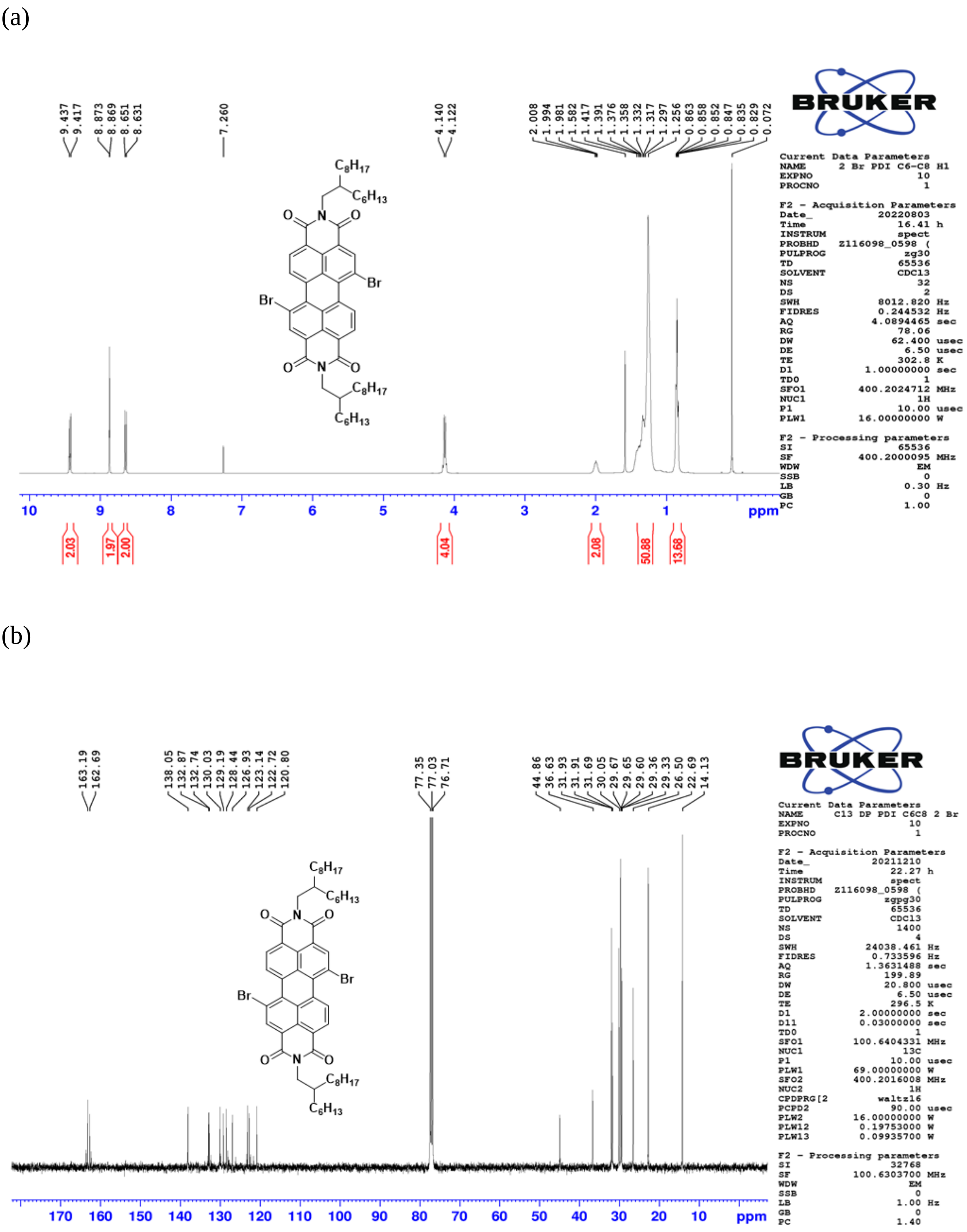

```
Current Data Parameters
NAME      2 Br PDI C6-C8 H1
EXPNO                    10
PROCNO                    1

F2 - Acquisition Parameters
Date_              20220803
Time                16.41 h
INSTRUM               spect
PROBHD    Z116098_0598 (
PULPROG                zg30
TD                    65536
SOLVENT               CDCl3
NS                       32
DS                        2
SWH                8012.820 Hz
FIDRES             0.244532 Hz
AQ                4.0894465 sec
RG                    78.06
DW                   62.400 usec
DE                     6.50 usec
TE                    302.8 K
D1               1.00000000 sec
TD0                       1
SFO1            400.2024712 MHz
NUC1                     1H
P1                    10.00 usec
PLW1            16.00000000 W

F2 - Processing parameters
SI                    65536
SF              400.2000095 MHz
WDW                      EM
SSB                       0
LB                     0.30 Hz
GB                        0
PC                     1.00
```

```
Current Data Parameters
NAME      C13 DP PDI C6C8 2 Br
EXPNO                    10
PROCNO                    1

F2 - Acquisition Parameters
Date_              20211210
Time                22.27 h
INSTRUM               spect
PROBHD    Z116098_0598 (
PULPROG              zgpg30
TD                    65536
SOLVENT               CDCl3
NS                     1400
DS                        4
SWH               24038.461 Hz
FIDRES             0.733596 Hz
AQ                1.3631488 sec
RG                   199.89
DW                   20.800 usec
DE                     6.50 usec
TE                    296.5 K
D1               2.00000000 sec
D11              0.03000000 sec
TD0                       1
SFO1            100.6404331 MHz
NUC1                    13C
P1                    10.00 usec
PLW1            69.00000000 W
SFO2            400.2016008 MHz
NUC2                     1H
CPDPRG[2            waltz16
PCPD2                 90.00 usec
PLW2            16.00000000 W
PLW12            0.19753000 W
PLW13            0.09935700 W

F2 - Processing parameters
SI                    32768
SF              100.6303700 MHz
WDW                      EM
SSB                       0
LB                     1.00 Hz
GB                        0
PC                     1.40
```

Figure S4. (a) ^1H- and (b) ^{13}C-NMR spectra of monomer M3 in $CDCl_3$.

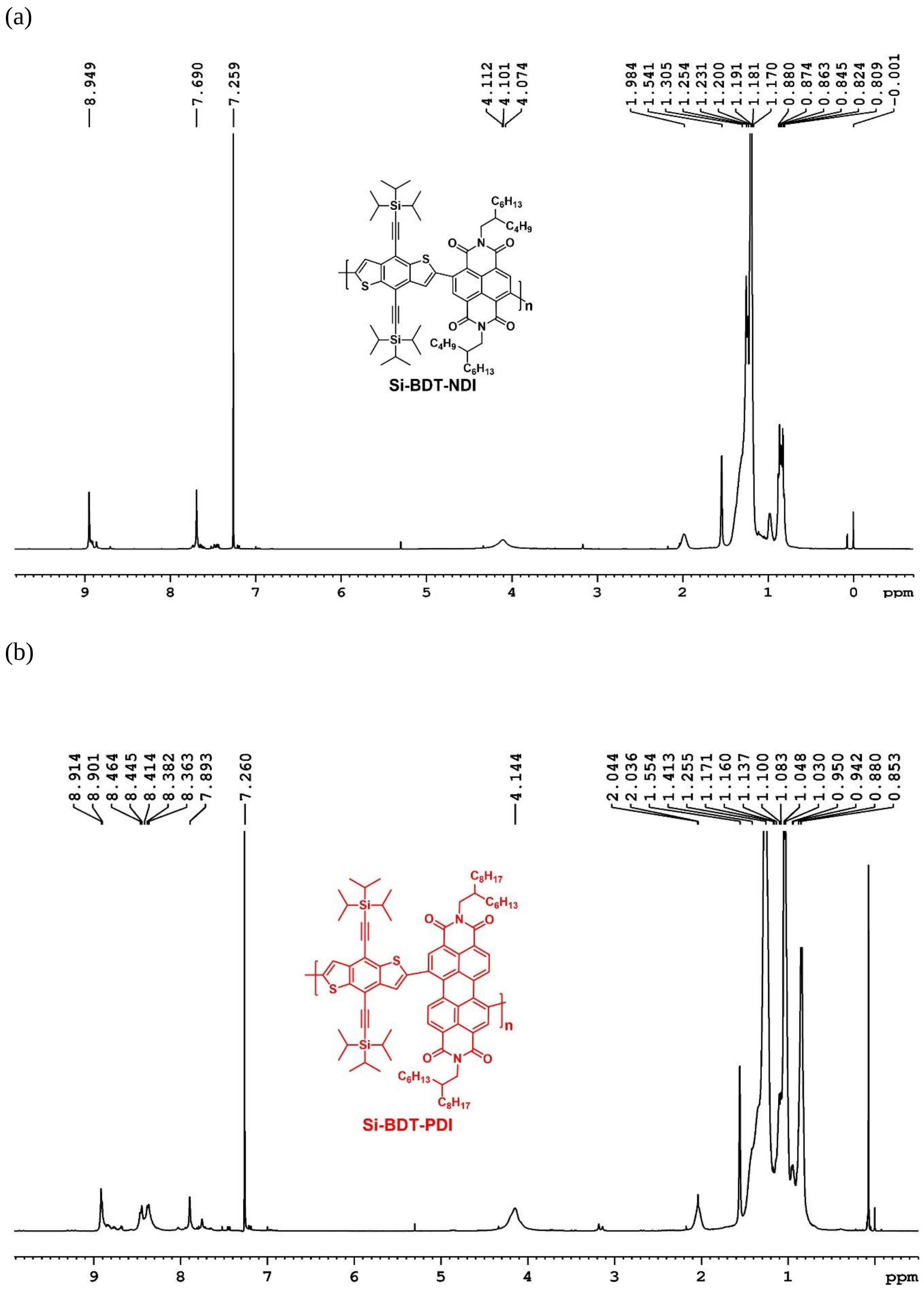

Figure S5. (a) ^{1}H- NMR spectra of polymer (a) **Si-BDT-NDI** and (b) **Si-BDT-PDI** in $CDCl_3$.

(a)

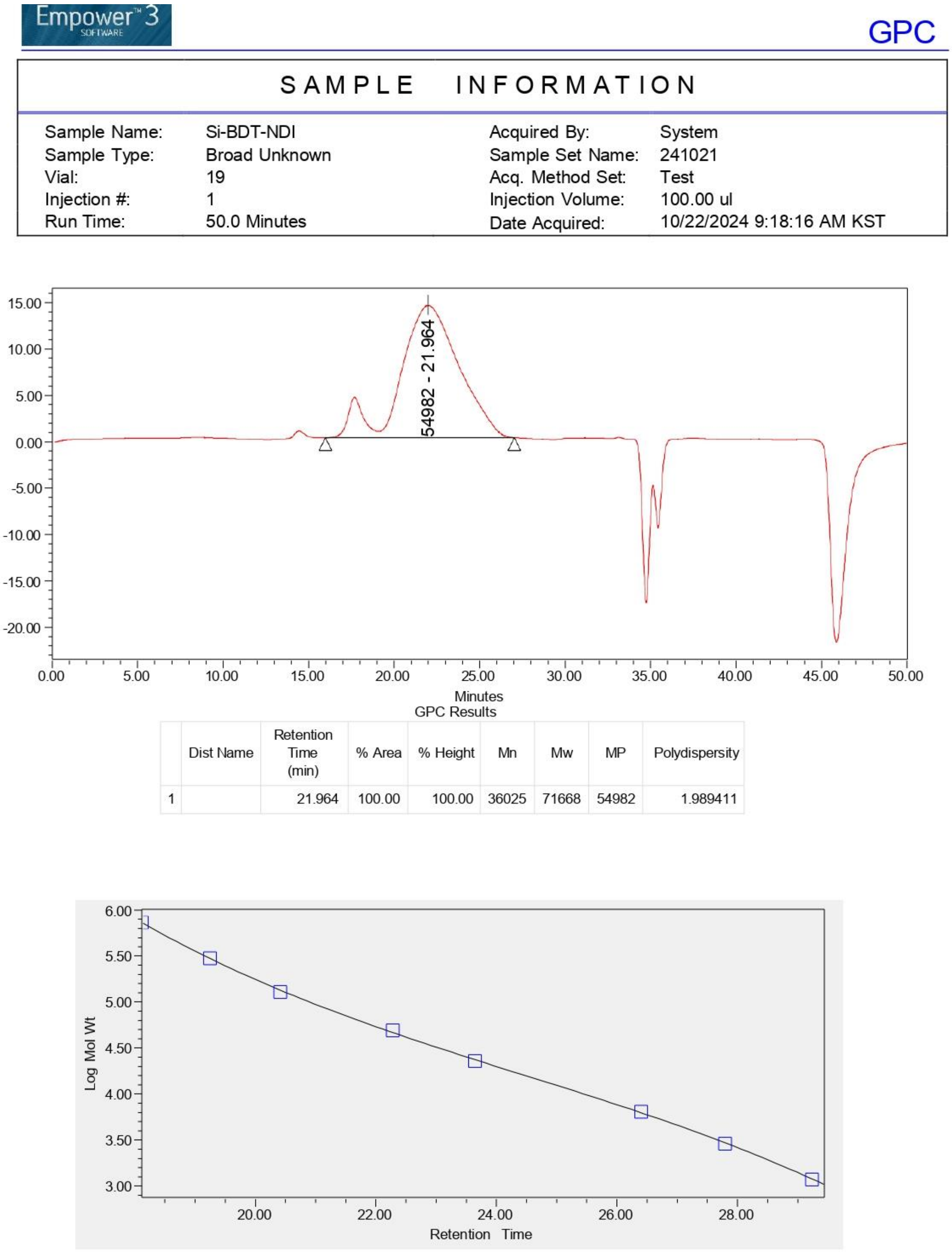

Empower™ 3 SOFTWARE

GPC

SAMPLE INFORMATION

Sample Name:	Si-BDT-NDI	Acquired By:	System
Sample Type:	Broad Unknown	Sample Set Name:	241021
Vial:	19	Acq. Method Set:	Test
Injection #:	1	Injection Volume:	100.00 ul
Run Time:	50.0 Minutes	Date Acquired:	10/22/2024 9:18:16 AM KST

GPC Results

	Dist Name	Retention Time (min)	% Area	% Height	Mn	Mw	MP	Polydispersity
1		21.964	100.00	100.00	36025	71668	54982	1.989411

(b)

GPC

SAMPLE INFORMATION

Sample Name:	Si-BDT-PDI	Acquired By:	System
Sample Type:	Broad Unknown	Sample Set Name:	241021
Vial:	18	Acq. Method Set:	Test
Injection #:	1	Injection Volume:	100.00 ul
Run Time:	50.0 Minutes	Date Acquired:	10/22/2024 8:27:01 AM KST

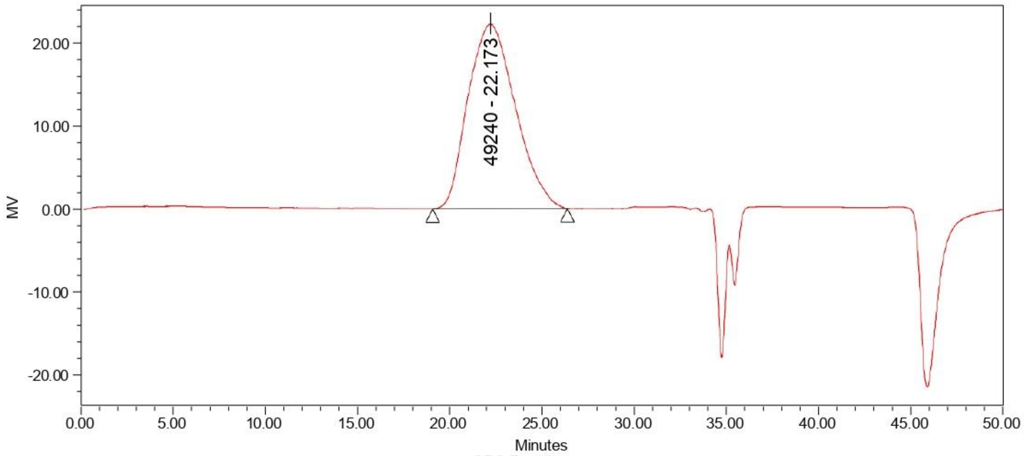

GPC Results

	Dist Name	Retention Time (min)	% Area	% Height	Mn	Mw	MP	Polydispersity
1		22.173	100.00	100.00	38001	54758	49240	1.440969

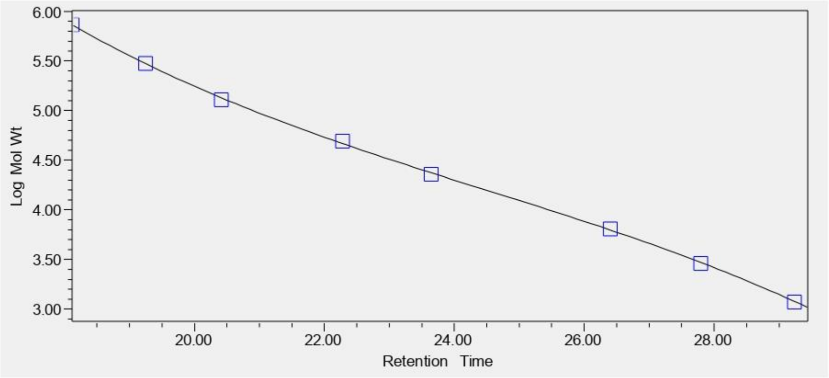

Figure S6: The molecular weights of the (a) Si-BDT-NDI, (b) Si-BDT-PDI polymers measured by gel permeation chromatography (GPC).

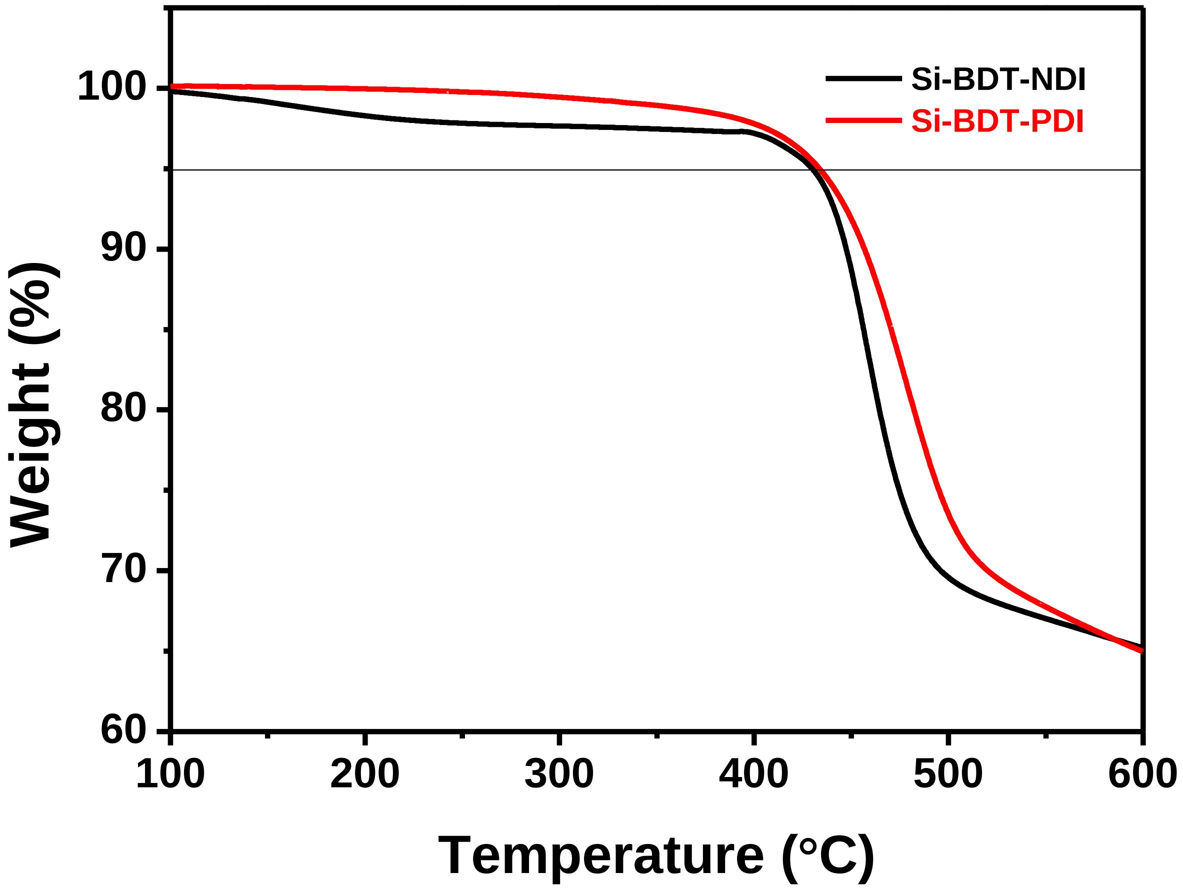

Figure S7. TGA thermograms of copolymers **Si-BDT-NDI**, and **Si-BDT-PDI** under N_2 flow at 10 °C min^{-1}.

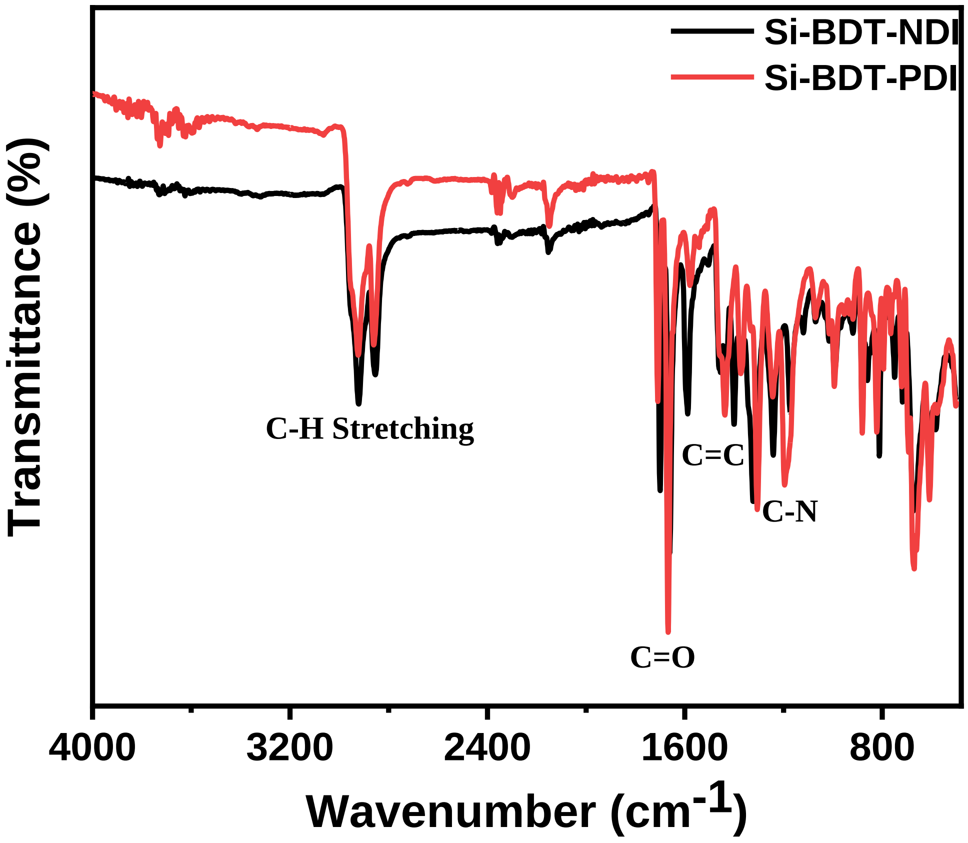

Figure S8. FTIR of **Si-BDT-NDI** and **Si-BDT-PDI** polymers.

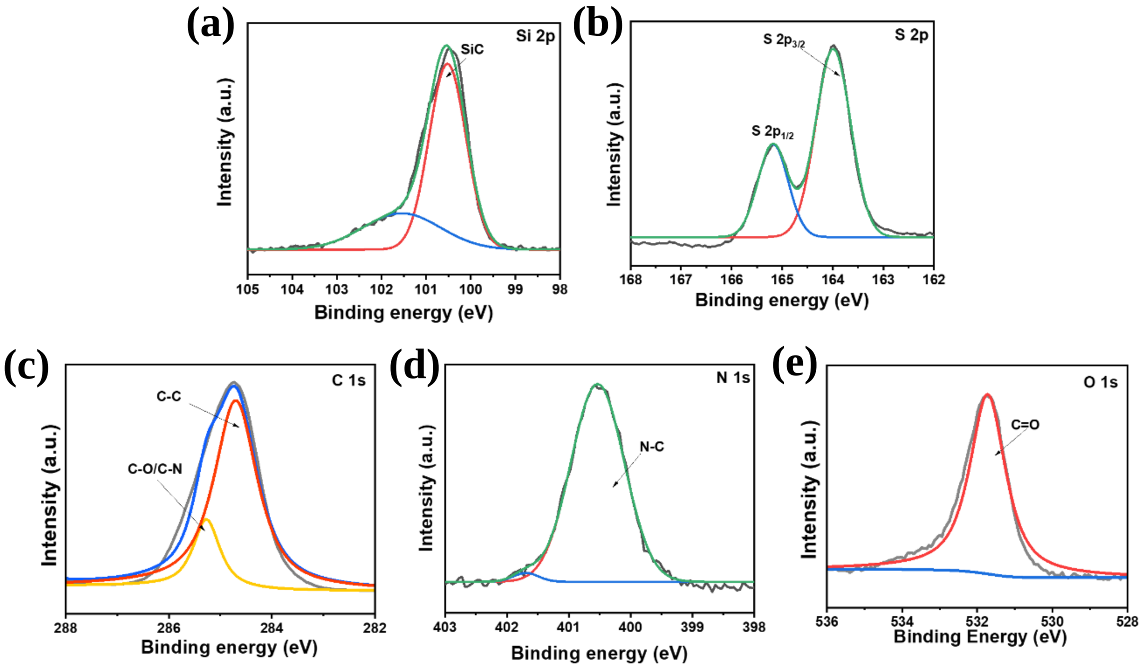

Figure S9. Deconvoluted spectra of (a) Si 2p, (b) S2p,. (c) C1s, (d) N1s, (e) O1s

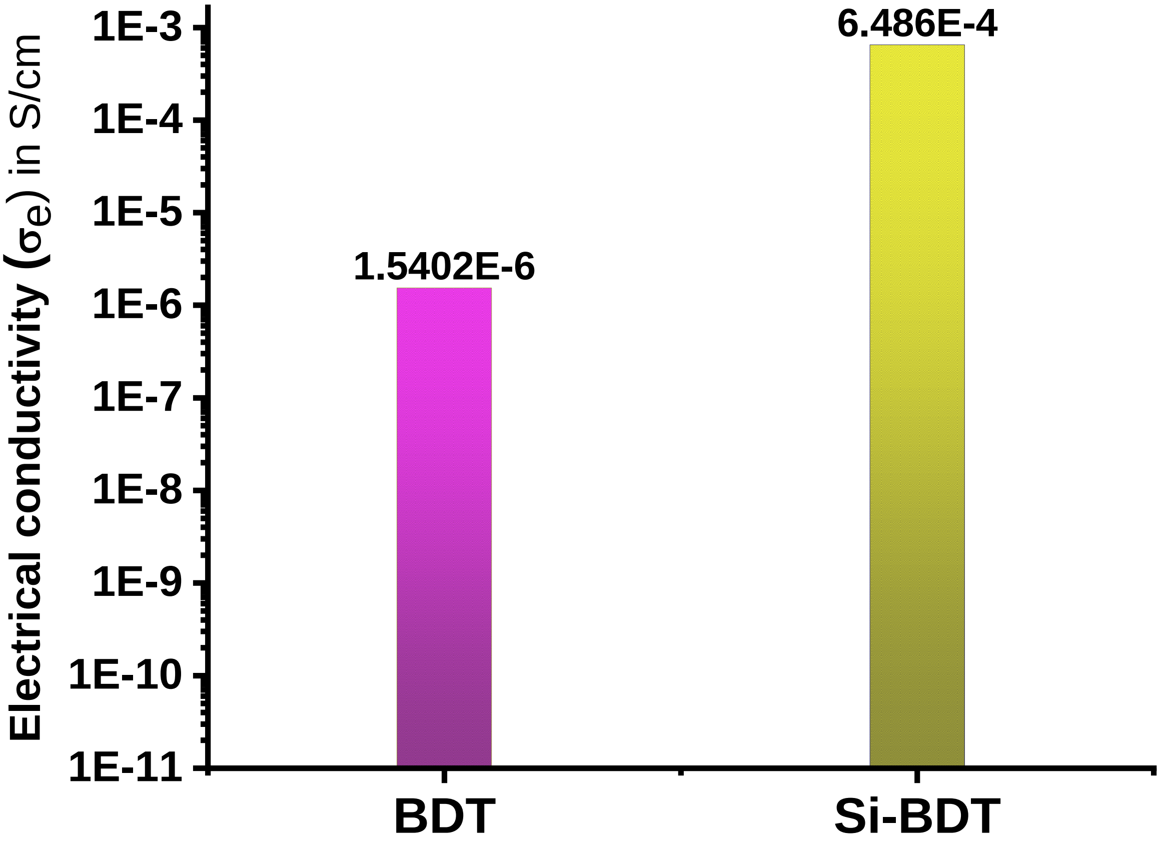

Figure S10. Electrical conductivity of BDT vs Si-BDT.

The electrical conductivity (σ_e) is calculated according to equation S5, where L is the length of the electrode (1.13mm), V is the applied voltage (1V), A is the total surface area (1cm^2), and I_e is the current obtained from the I–V test.

$$\sigma_e = {}^{LI_e}\!/_{VA} \tag{S5}$$

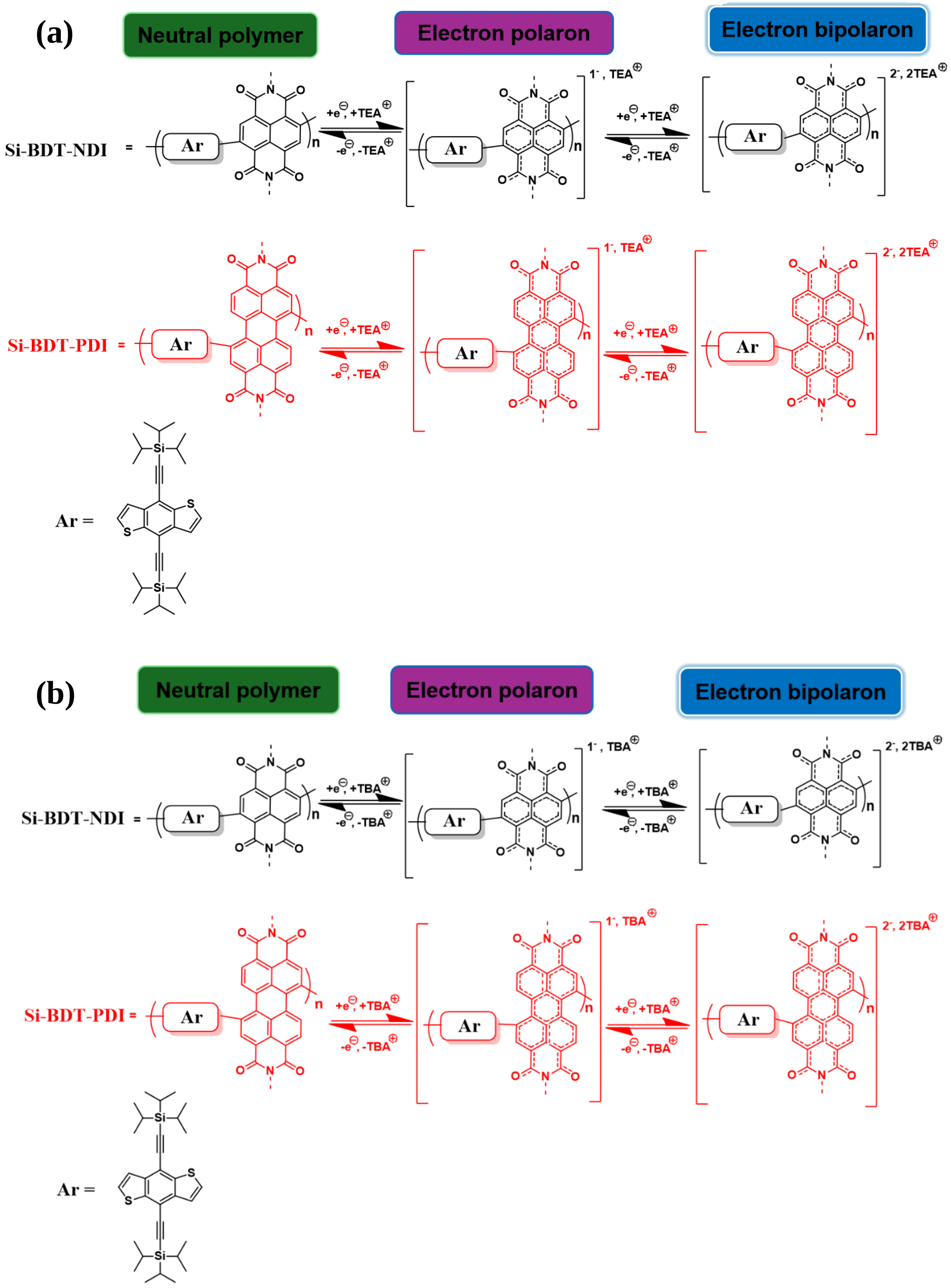

Figure S11. Schematic representation of the proposed plausible reversible redox reaction mechanism of n-type pseudocapacitive electrodes, Si-BDT-NDI and Si-BDT-PDI in (a) $TEABF_4$ (b) $TBAPF_6$ electrolytes.

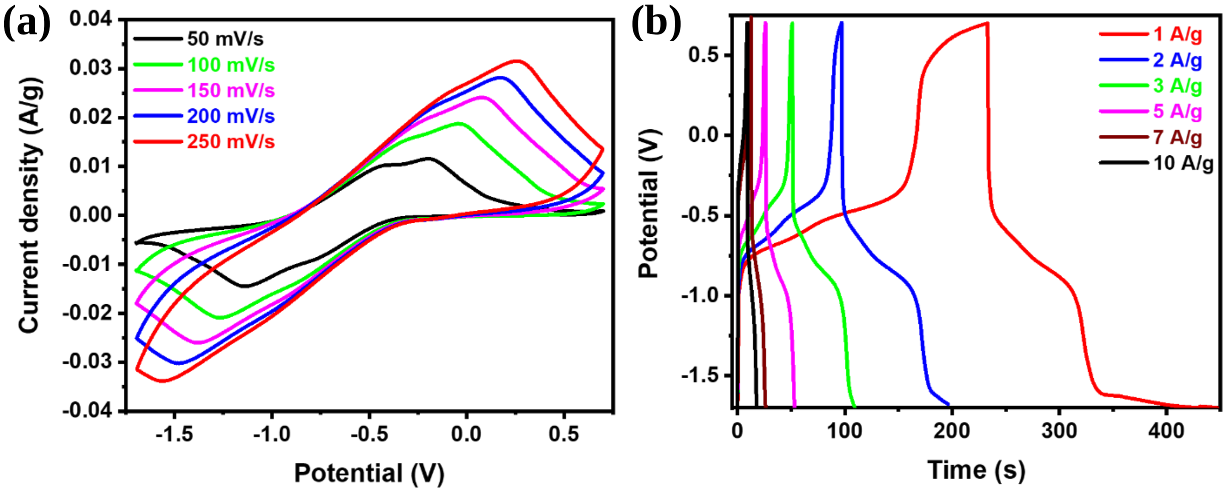

Figure S12. Three electrode electrochemical performance of **Si-BDT-NDI** (a) CV and (b) GCD in 0.1M TBAPF$_6$.

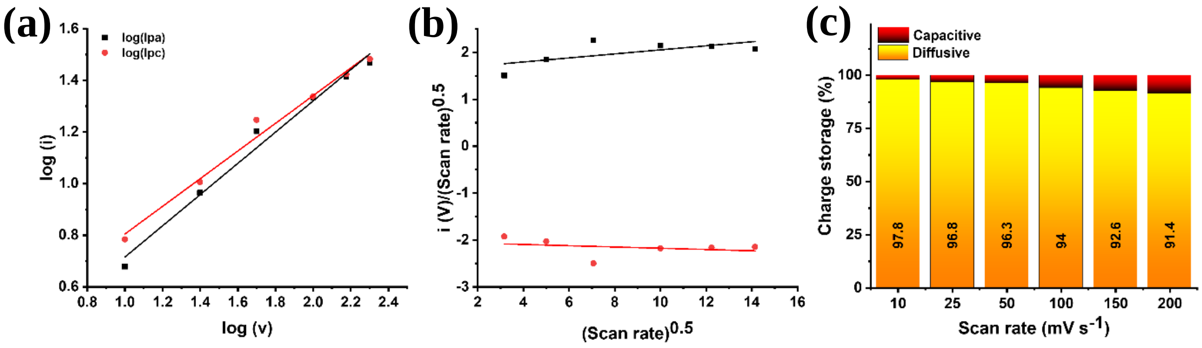

Figure S13. (a) linear relationship between the logarithmic peak current and logarithmic scan rate i.e., log(i) *vs* log (ν), (b) linear fit plot between (scan rate)^{½} and i(ν)/(scan rate)^{½}, and (c) Capacitive and diffusive charge storage contribution at various scan rates of 10-200 mV s^{-1}.

The power law approach is commonly employed to investigate the kinetic characteristics derived from cyclic voltammetry (CV) measurements at different potentials. The CV curves ranging from 10 to 200 mV s^{-1} (Fig. 3d) depict the involvement of the faradaic charge storage mechanism due to the redox activity of the electrode material. According to this method, the peak current (i) and scan rate (ν) are related by the equation:

$$i=a\nu^{b} \tag{S6}$$

In this expression, *a* and *b* are constants that vary depending on the scan rate at a given potential. The value of *b* is obtained from the slope of the linear plot of log(i) versus log(ν). A *b* value less than 1 suggests a diffusion-controlled process, whereas a value close to 1 indicates a capacitive mechanism.

In Figure S11a, the observed *b* values are approximately 0.53 in cathodic region and 0.6 in anodic region, suggesting signifying dominant diffusive behavior during the redox reactions. Ipa and Ica denotes peak anodic and cathodic current respectively.

The total current at a given potential can be deconvoluted into capacitive ($k_1\nu$) and diffusion-controlled ($k_2\nu^{1/2}$) contributions, as described by:

$$i(\nu) = k_1\nu + k_2\nu^{1/2} \tag{S7}$$

Rearranging this gives a linear form:

$$\frac{i(\nu)}{\nu^{1/2}} = k_1\nu^{1/2} + k_2 \tag{S8}$$

Plotting $i(\nu)/\nu^{1/2}$ against $\nu^{1/2}$ (as shown in Figure S11b) results in nearly straight lines with slight deviation for different potentials, where the slope corresponds to k_1 and the intercept to k_2. These parameters quantify the capacitive and diffusion-controlled charge storage, respectively.

Figure S11c highlights that the polymeric material exhibits a diffusive contribution of approximately 91% calculated in the cathodic region, indicative of fast ionic transport and surface redox activity. The remaining 9% is attributed tocapacitive, such as due to surface ion and electron adsorption, particularly evident at a high scan rate of 200 mV s^{-1}.

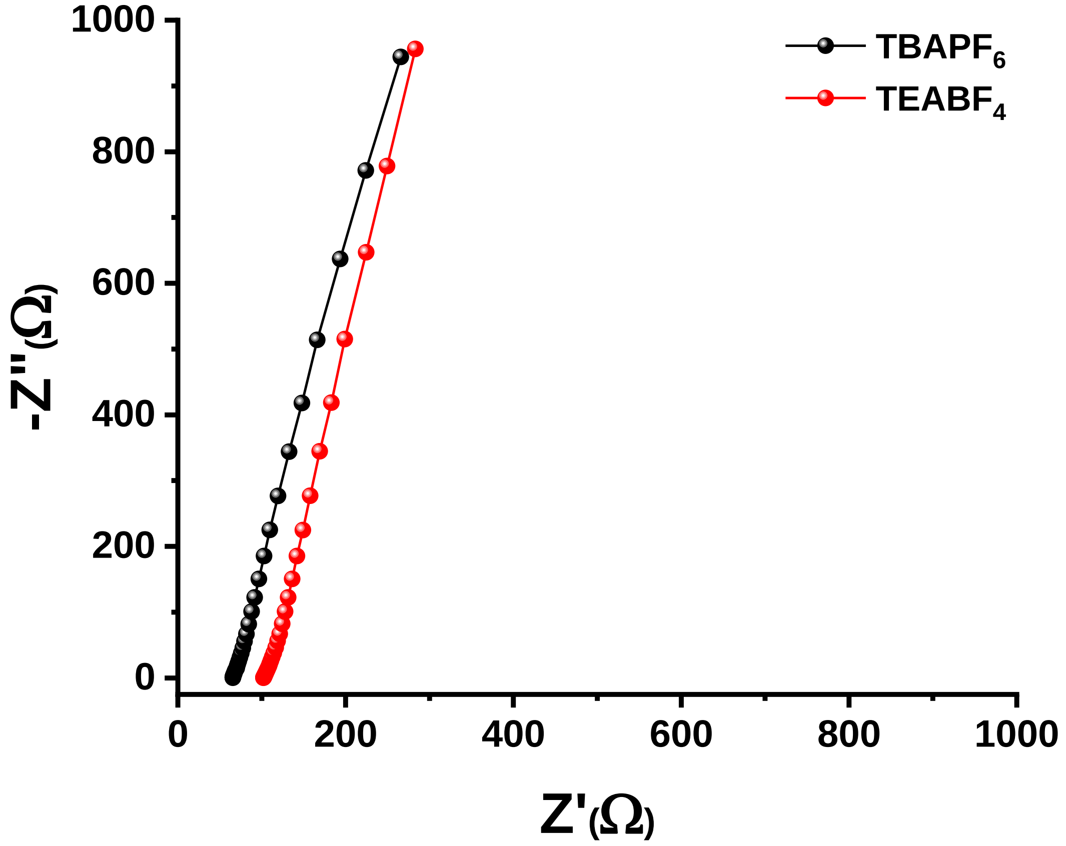

Figure S14. Nyquist impedance plot of two electrolytes for ionic conductivity measurement.

The ionic conductivity for the two used organic electrolytes was measured from the Nyquist impedance plot within the frequency range 10^6 Hz to 1 Hz at a small perturbation voltage of 10 mV. The electrochemical measurements were performed on an indigenously build cylindrical electrochemical cell consisting of two non-destructive Pt electrodes of 1cm*1cm size separated at a fixed distance of 1.5 cm. The conductivity (σ) of both the electrolytes was calculated using the following relation:

$$\sigma = \frac{1}{R}\frac{d}{S} \qquad \text{(S9)}$$

Where, R is resistance of the electrolytes from the impedance plot, d is the distance between two Pt electrodes and S is area of the electrodes. All the electrochemical impedance measurements were performed at room temperature.

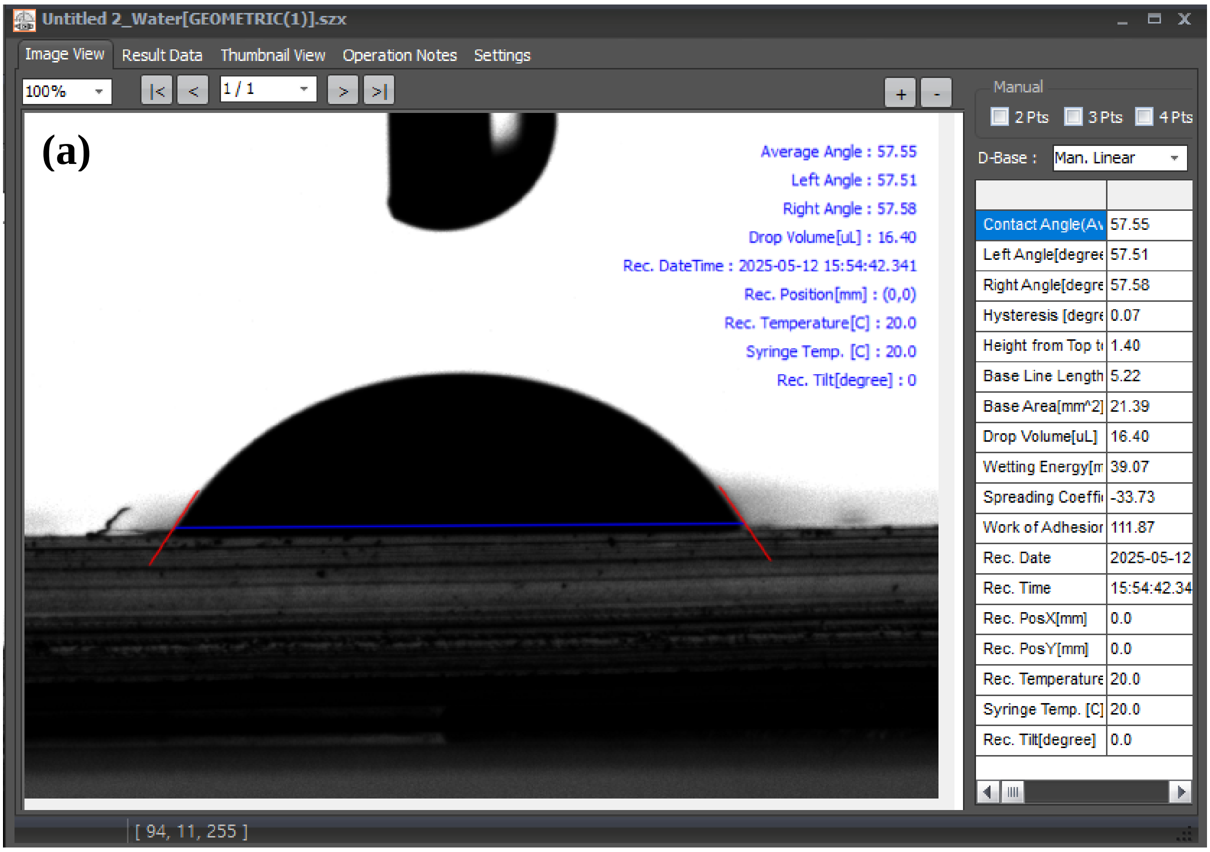

Average Angle : 57.55
Left Angle : 57.51
Right Angle : 57.58
Drop Volume[uL] : 16.40
Rec. DateTime : 2025-05-12 15:54:42.341
Rec. Position[mm] : (0,0)
Rec. Temperature[C] : 20.0
Syringe Temp. [C] : 20.0
Rec. Tilt[degree] : 0

D-Base : Man. Linear

Contact Angle(Av	57.55
Left Angle[degree	57.51
Right Angle[degre	57.58
Hysteresis [degre	0.07
Height from Top t	1.40
Base Line Length	5.22
Base Area[mm^2]	21.39
Drop Volume[uL]	16.40
Wetting Energy[m	39.07
Spreading Coeffi	-33.73
Work of Adhesior	111.87
Rec. Date	2025-05-12
Rec. Time	15:54:42.34
Rec. PosX[mm]	0.0
Rec. PosY[mm]	0.0
Rec. Temperature	20.0
Syringe Temp. [C]	20.0
Rec. Tilt[degree]	0.0

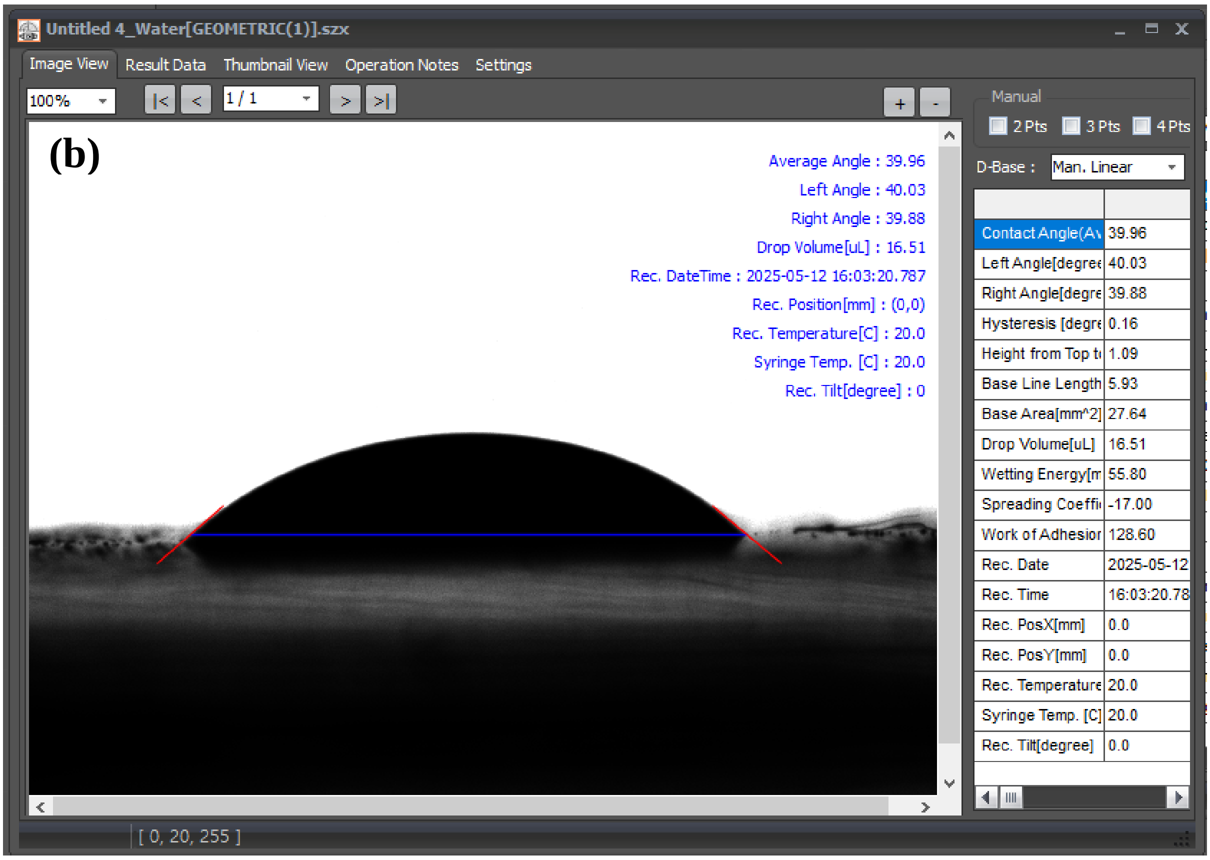

Average Angle : 39.96
Left Angle : 40.03
Right Angle : 39.88
Drop Volume[uL] : 16.51
Rec. DateTime : 2025-05-12 16:03:20.787
Rec. Position[mm] : (0,0)
Rec. Temperature[C] : 20.0
Syringe Temp. [C] : 20.0
Rec. Tilt[degree] : 0

D-Base : Man. Linear

Contact Angle(Av	39.96
Left Angle[degree	40.03
Right Angle[degre	39.88
Hysteresis [degre	0.16
Height from Top t	1.09
Base Line Length	5.93
Base Area[mm^2]	27.64
Drop Volume[uL]	16.51
Wetting Energy[m	55.80
Spreading Coeffi	-17.00
Work of Adhesior	128.60
Rec. Date	2025-05-12
Rec. Time	16:03:20.78
Rec. PosX[mm]	0.0
Rec. PosY[mm]	0.0
Rec. Temperature	20.0
Syringe Temp. [C]	20.0
Rec. Tilt[degree]	0.0

Figure S15. Contact angle of two electrolytes a) $TEABF_4$, b) $TBAPF_6$ on PDMS substrate.

Table S1. HOMO and LUMO energy levels, along with the HOMO-LUMO energy gap (ΔE_g) (in eV), for **Si-BDT-NDI** and **Si-BDT-PDI** in the presence of electrolytes $TEABF_4$ and $TBAPF_6$ calculated at the B3LYP-D3/6-31G(d,p) level of theory.

	E_{HOMO} (eV)	E_{LUMO} (eV)	ΔE_g (eV)
Si-BDT-NDI & $TEABF_4$	-5.60	-3.32	2.28
Si-BDT-PDI & $TEABF_4$	-5.60	-3.35	2.25
Si-BDT-NDI & $TBAPF_6$	-5.60	-3.45	2.15
Si-BDT-PDI & $TBAPF_6$	-5.63	-3.51	2.12

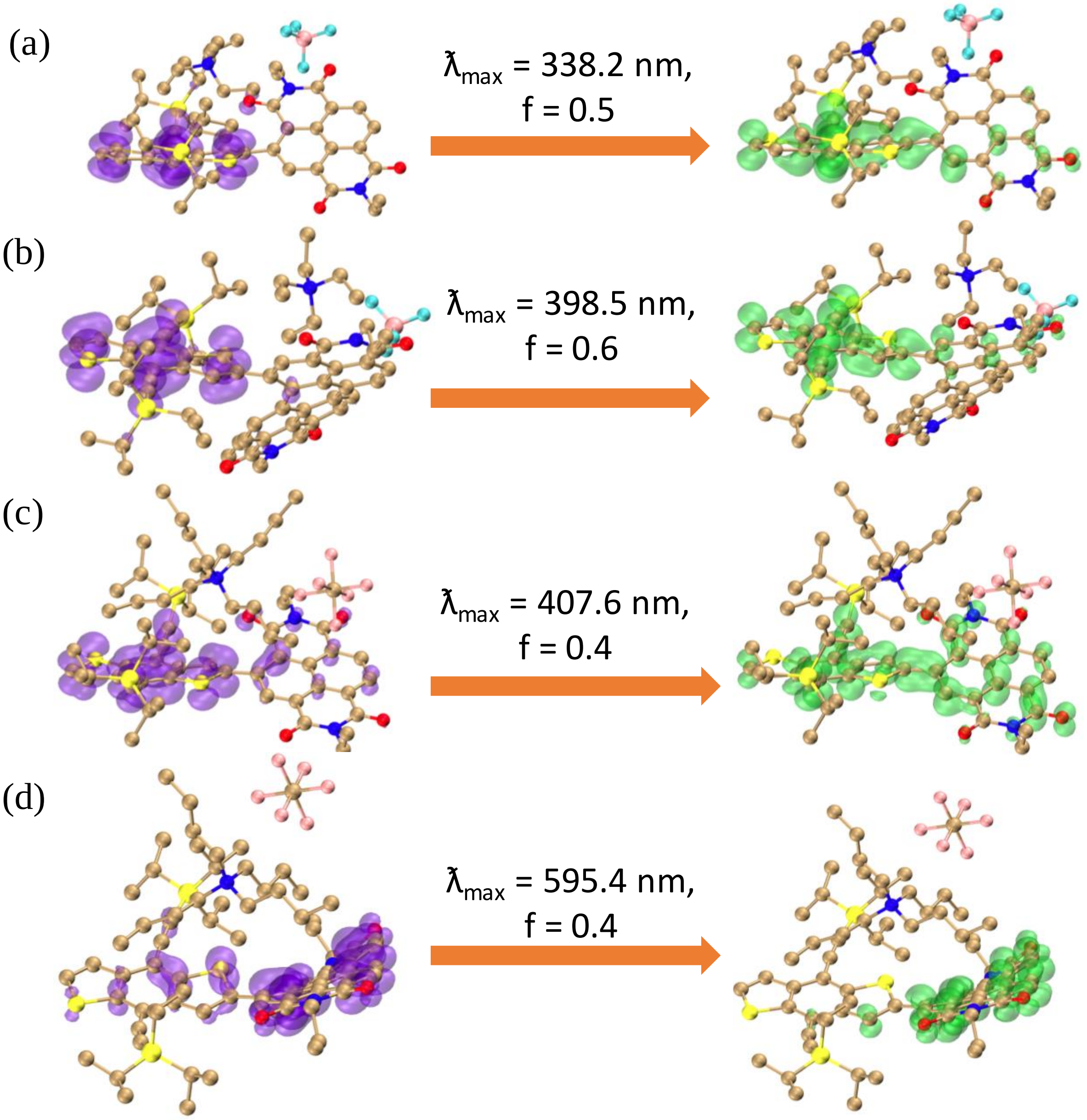

Figure S16. Natural transition orbitals (NTO) corresponding to the characteristic UV-Vis absorption in (a) Si-BDT-NDI & $TEABF_4$, (b) Si-BDT-PDI & $TEABF_4$, (c) Si-BDT-NDI & $TBAPF_6$, and (d) Si-BDT-PDI & $TBAPF_6$. For each NTO, the hole (purple) and electron (green) orbitals are given on the left and right, respectively. The calculated transition wavelength (λ_{max}) and oscillator strength (f) for each transition are shown.

Based on the NTO analysis, $TBAPF_6$ appears to interact more efficiently with the **Si-BDT-NDI/PDI** electrode (Figures S14 c and d), as it allows for delocalization of both hole and electron over the entire electrode structure. In contrast, $TEABF_4$ causes the hole and electron to stay localized on the Si-BDT moiety (Figures S14 a and b), thus reducing charge distribution within the electrode and limiting the charge transfer to the **Si-BDT-NDI/PDI** system. This showsthat $TBAPF_6$ likely enhances the charge transfer efficiency and electronic interaction across the **Si-BDT-NDI/PDI** electrode.

These interactions, highlighted by bond paths (orange lines), connecting the BCPs further validate the electrostatic and van der Waals interactions within the hydrophobic regions of the Si-BDT backbone**,** particularly between the bulky alkyl groups of TEA^+ or TBA^+ and the π-conjugated framework of the electrode, thereby stabilizing the electrode-electrolyte interface and enhancing structural integrity and charge transfer. Cage critical points (CCPs), denoted by green dots, emerge in regions of spatial confinement, particularly within the complex electrode-electrolyte arrangements. These points indicate areas of enclosed electron density, reflecting steric and electrostatic influences that dictate the molecular organization of the electrolyte ($TEABF_4$ or $TBAPF_6$) around the electrode surface or Si-BDT framework.

The AIM analysis further supports the superior stability of the Si-BDT-PDI & $TBAPF_6$ system compared to other studied systems, as evidenced by a denser network of non-covalent interactions compared to $TEABF_4$. The stronger π-ion interactions and enhanced charge transfer efficiency observed in this system contribute to its higher electrochemical stability and improved supercapacitor performance, aligning with the NCI analysis findings.

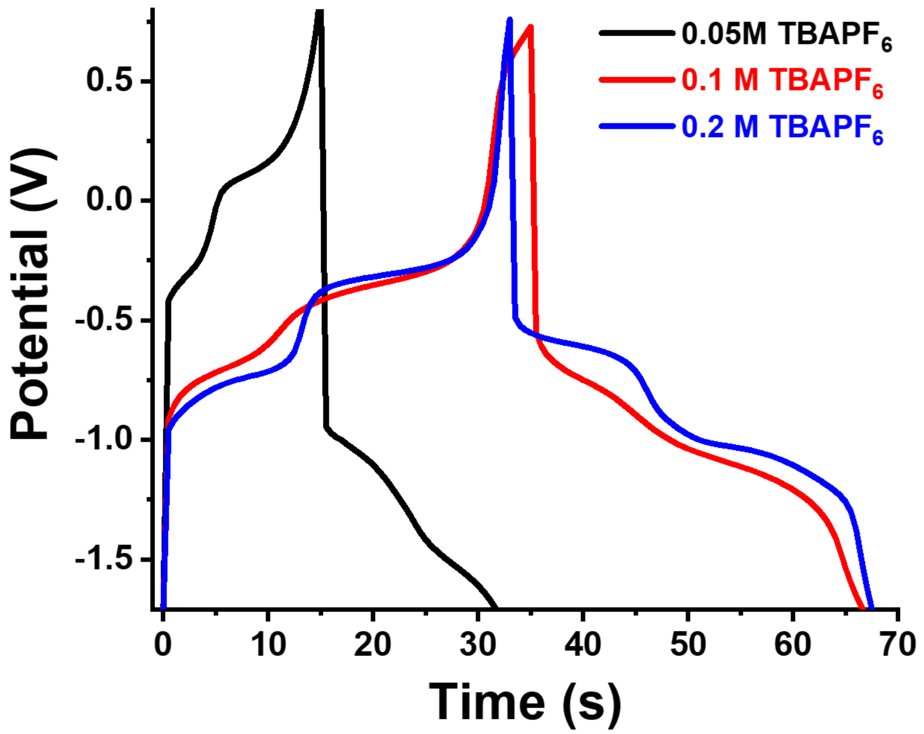

Figure S17. Three electrode electrochemical performance of **Si-BDT-PDI** with 0.05, 0.1 and 0.2 M TBAPF$_6$ electrolyte.

The use of 0.1 M electrolyte concentration was originally selected to achieve an optimal balance between ionic conductivity, electrochemical stability, and viscosity, in line with established literature. At lower concentrations (e.g., 0.05 M), reduced ion availability hampers efficient charge transport, resulting in a noticeable drop in specific capacity as well as IR drop. In contrast, at higher concentrations (e.g., 0.2 M), while ionic conductivity may initially increase, the concurrent rise in viscosity and enhanced ion pairing can limit ion mobility and diminish rate performance. Our measurements show that even after doubling the concentration from 0.1 M to 0.2 M, the increase in specific capacity (Csp) is marginal, indicating saturation of the beneficial effect. These observations are consistent with previously reported findings in non-aqueous supercapacitor systems, where intermediate concentrations are known to minimize resistance and facilitate optimal charge transfer kinetics. [S6-7]

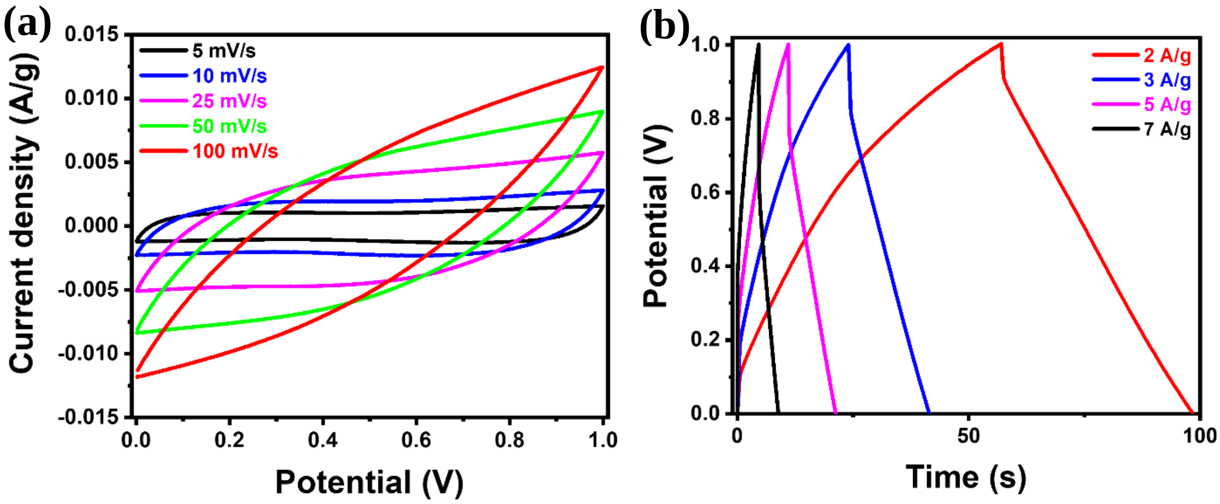

Figure S18. PAC electrochemical performance in 0.1M $TBAPF_6$.

Reference:

[S1] S .K. Pati, D. Patra, S. Muduli, S. Mishra, S. Park, Small 2023, 19, 2300689.

[S2] H. Zhang, S. Zhang, K. Gao, F. Liu, H. Yao, B. Yang, C. He, T.P. Russell, J. Hou, J. Mater. Chem. A 2017, 5, 10416–10423.

[S3] Z. Zhao, Z. Yin, H. Chen, L. Zheng, C. Zhu, L. Zhang, S. Tan, H. Wang, Y. Guo, Q. Tang, Y. Liu, Adv. Mater 2017, 29 1602410.

[S4] S. Sharma, R. Soni, S. Kurungot, S.K. Asha, J. Phys. Chem. C 2019, 123, 2084-2093.

[S5] D. Pandey, M. K. Singh, S. Mishra, D. K. Rai and A. Raghuvanshi, J. Mater. Chem. A 2024, 12, 27355–27363.

[S6] M. Vijayakumar, D. S. Rohita, T. N. Rao, M. Karthik, Electrochimica Acta, 2019, 298, 3 47-359.

[S7] S. Haldar, D. Rase, P. Shekhar, C. Jain, C. P. Vinod, E. Zhang, L. Shupletsov, S. Kaskel and R. Vaidhyanathan, Advanced Energy Materials, 2022, 12, 2200754.